Development of a microfluidic rolling circle amplification module for bacterial detection

Rafaela Rodrigues Rosa [1]
[1]rafaela.rosa@tecnico.ulisboa.pt

Instituto Superior Técnico,Lisboa Portugal
November 2021

Abstract

Antibiotic resistance has been a growing health concern for the past decades. The inability to kill or inhibit these resistant bacteria from proliferating has made it very challenging to treat such infections. In order to prevent these infections from spreading, it is necessary to have fast and accurate diagnostic methods.

The field of microfluidics provides an excellent platform for this type of device, particularly for point-of-care platforms, due to its advantages such as reduced size and higher surface-to-volume ratio, as well as reduced fabrication cost. In this work, a microfluidic rolling circle amplification (RCA) module for bacterial detection, using *Staphylococcus Aureus* as a bacterial model was developed. This device uses a microfluidic channel packed with streptavidin beads to which a probe DNA will bind to through a streptavidin-biotin bond and hybridize with a padlock. The target DNA to be detected will then hybridize to this padlock and be amplified through RCA. The assay was optimized regarding several aspects, such as the flow rates. The target DNA capture was also performed under several saline conditions, and it was verified that it was possible to capture it under all the tested conditions. The target DNA capture was quantified with capture efficiencies ranging from 27% to 77%, and through the rolling circle amplification, it was only possible to detect 1% of the amplified products.

Key Words: Antibiotic resistance**,** *Staphylococcus Aureus***,** rolling circle amplification, microfluidic system

1. Introduction

Antimicrobial resistance has been a growing health concern for the past decades, almost since its discovery in the 1900's. It is currently one of the most significant global public health challenges, threatening the ability to effectively treat an ever-growing range of infections caused by bacteria, viruses, or fungi. [1] [2] [3]

One of the main ways antibiotic resistance is introduced and spread is in the healthcare setting, such as in hospitals, through patients or health care workers from the outside or other institutions, from patients transferred to or from extended care facilities, or through contaminated products. This is mainly due to selection pressure by antibiotic use and made worse by its inappropriate and over usage, such as inadequate dosing, and excessive or improper prescription by physicians. With the spread of antibiotic resistance, many organisms that were previously susceptible to antibiotics have acquired resistance. That is the case for *S. Aureus*, as the first strains of Methicillin-resistant *Staphylococcus Aureus* (MRSA) emerged in the 1960s, mostly related to elderly and immunocompromised patients, and like most antibiotic-resistant bacteria, then spread to the community. The insertion of the mecA gene in the accessory component of the *S. Aureus* genome in the staphylococcal chromosomal cassete mec causes this resistance to methicillin, which further complicates the treatment of *S.Aureus* infections. In the 2019 CDC's report of Antibiotic Resistance Threats in the United States, MRSA was declared a serious threat, and it was estimated that approximately 323,700 hospitalized patients contracted a MRSA infection, and around 10,600 resulted in deaths. [1] [2] [3] [4] [5] [6]

Due to the increased health burden caused by these types of infections, one way to prevent the spread of antibiotic-resistance is through rapid pathogen detection devices, which would allow to reduce the exposure to broad-spectrum antibiotics, as well as implementing pathogen targeted therapy. Point-of-care (POC) platforms that are sensitive, accurate, easy to use and interpret, portable, disposable, require small sample volumes, are stable under a wide range of conditions, have a rapid turnaround time, and remain cost-effective would allow for testing at or near the site of patient care, providing a prompt diagnosis and appropriate treatment, thus preventing and stopping the antimicrobial resistance problem. [7] [8] [9] [10] [11]

The field of microfluidics provides an excellent platform for POC devices, due to its advantages such as reduced size, higher surface-to-volume ratio and reduced fabrication costs. Several new microfluidic devices have been developed capable of outperforming the classically used techniques in several areas of research, such as food and environmental monitoring [12] [13], biological assays, such as cell counting and cell

culture [14], and health diagnostics. [15] Therefore, given that DNA based detection is a powerful tool for diagnostics due to its precision and accuracy, moving it from centralized laboratories to POC platforms would allow for faster and more cost-effective diagnostic tools. Several nucleic acid amplification microfluidic devices for pathogen detection have been developed, taking advantage of the reduced size allowing for faster reaction times, less reagent and sample consumption, as well as a more precise temperature control due to rapid heat conduction. [16] [17]. Some of these platforms integrate the standard PCR technique for nucleic acid amplification [18] but most often employ isothermal amplification techniques such as LAMP or RCA [19] [20] [21] that overcome the intrinsic disadvantage of PCR that requires a thermal cycler.

Throughout this work, a microfluidic rolling circle amplification module for bacterial detection was developed. The reaction occurs at a constant temperature of 37℃, requiring solely a circular DNA template termed padlock (PLP), a short DNA or RNA primer/target and a DNA polymerase to start the reaction, generating a long single-stranded molecule containing thousands of repeated copies of the circular template tethered to the original circular DNA. [16][22][23] The system was optimized regarding several aspects, including flow rates and the influence of the saline conditions on the target DNA capture. Quantification of the target DNA captured using this system was also done, with capture efficiencies ranging from 27% to 77% for concentrations of 250nM and 50nM, respectively. Through the rolling circle amplification, it was possible to detect 1% of the amplified products. The final goal would be to capture and amplify DNA from a real sample of *Staphylococcus Aureus.*

2. Materials and Methods

2.1 Microfluidic Device Fabrication

The microfluidic devices used throughout this work were comprised of channels with two different heights, 100μm and 20μm to allow the entrapment of the beads. The Polydimethylsiloxane (PDMS) devices were fabricated using a soft-lithography technique described in detail elsewhere [24]. To obtain the SU-8 master mold used for the device fabrication two hard masks were fabricated, one for each height feature. Firstly, the two aluminum hard masks were fabricated by depositing a 2000Å layer of aluminum by magnetron sputtering (Nordiko 7000) onto a glass substrate (Corning Eagle glass). Following this, the hard mask design is patterned by a Direct Writing Lithography system (DWL 2.0, Heidelberg systems) and chemical wet etching (TechniEtch A180 Aluminium etchant, Microchemicals). The hard masks are then used to create an SU-8 master mold. The 20μm layer was fabricated by spin-coating an SU-8 2015 (Microchem) layer on top of a silicon substrate followed by UV-light exposure, through the first hard mask, and development in a propylene glycol monomethyl ether acetate (PGMEA) 99% solution (Sigma-Aldrich). Next, a 100μm thick layer of SU-8 is spin-coated on top of the first layer and the second hard-mask is manually aligned with the previous structure, followed again by UV-light exposure, development in a PGMEA solution and undergoing a final hard-bake for 15min at 150 ℃.

The SU-8 mold is then used to fabricate the PDMS structures. Firstly, a mixture of curing agent and PDMS (Sylgard 184 silicon elastomer kit, Dow-Corning) was prepared in a weight ratio of 1:10 and poured on top of the previously fabricated SU-8 master mold, fixed on a poly(methyl methacrylate) (PMMA) frame and placed in the oven at 70℃ for 90min to cure. After removing the cured PDMS from the oven, the structure was removed from the frame, and holes were punched in the inlets and outlets of the columns. The microfluidic structure is then sealed against a 500μm thick PDMS membrane after treatment with oxygen plasma (Harrick Plasma PDC-002-CE).

2.2 DNA Oligonucleotides and Beads

All DNA oligonucleotide sequences used throughout this work are described in Table 1. The padlock probe, padlock and complementary target ssDNA were purchased from Integrated DNA Technologies (Leuven, Belgium) and the non-complementary target ssDNA sequences were purchased from Stabvida Genomics Lab (Caparica, Portugal). The detection oligonucleotides non-complementary to the padlock probe were acquired from Eurogentec (Seraing,Belgium), and the remaining oligonucleotide sequences were graciously provided by the SciLifeLab (Sweden). All DNA oligonucleotide sequences were kept in 100μM aliquots and stored at -20℃ until further usage, at which point they were serial diluted with PBS to the concentrations used in the assays, with the exception of the detection oligonucleotides, which were diluted in hybridization Buffer.

Along this work two types of beads, Q-Sepharose and streptavidin agarose beads, were used to immobilize the DNA. The Q-Sepharose ™ Fast Flow

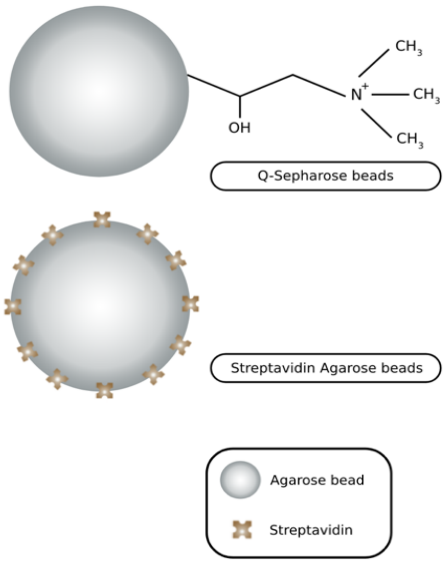

Figure 1: *Schematic representation of the surface functionalization of the Q-Sepharose and streptavidin beads.*

Table 1: *Summarized list of the oligonucleotides sequences used in this work, as well as their modifications (mod).*

Oligonucleotides	Sequence (5'-3')	5' mod	3' mod
Padlock probe	TTTTTTTTTTGTAAGACACTATTACTGAGGA	Biotin	none
Padlock	TGCTTTGTTTCAGGTGTAGTGTATGCAGCTCCTCAGTAATAGTGTCTTACGGCATCACTGGTTACGTCTGTCTCTACACCTTTTTTAGGA	PO4-phosphorilation	none
Complementary target ssDNA	TTAAATTAATGTACAAAGGTCAACCAATGACATTCAGACTATTATTGGTTGATACACCTGAAACAAAGCATCCTAAAAAAGGTGTAGAGA	Atto-430LS	none
Biotinylated Detection Oligonucleotides	AAAAAAAAAACATTCTGTGATAATGACTCCT	Biotin	none
Non-complementary target ssDNA	CGTGTCGTTCACATCTGTCCGT	Atto-430LS	none
Non-complementary target ssDNA	TCGCGACATTCATTATGCCCAATTTTTAA	Atto-430LS	none
Complementary target ssDNA	TTAAATTAATGTACAAAGGTCAACCAATGACATTCAGACTATTATTGGTTGATACACCTGAAACAAAGCATCCTAAAAAAGGTGTAGAGA	none	none
Detection Oligonucleotides (complementary to padlock probe)	AAAAAAAAAACATTCTGTGATAATGACTCCT	Cy3	none
Detection Oligonucleotides	GGCATCACTGGTTACGTCTGTTTT	Cy3	none
Detection Oligonucleotides	GGCATCACTGGTTACGTCTGTTTT	Atto-430LS	none

beads were purchased from GE Healthcare Bio-Sciences and kept as a slurry in 20% ethanol. The Streptavidin Agarose beads were purchased from EMD Milipore Corp USA, and also kept as a slurry in 20% ethanol.

2.3 Microfluidic Handling and Bead Packing

To pack the columns, a pumping system, comprised of a syringe pump (New Era Pump Systems, Inc.) was used. The syringes were connected to the microfluidic structures through tubing and metal adaptors at the outlets, and the bead solutions were flown through the channel by placing a pipette tip with the desired bead solution at the inlet and pulling the solution from the outlet, using a flow rate of 5μL/min, creating negative pressure inside the column.

To flow the remaining solutions through the microfluidic channel, the same pumping system was used. The syringes were connected to tubing and metal adaptors and filled with PBS, followed by an air gap, before the desired solution was pulled into the tubing. Instead of pulling, the liquids were pushed inside the syringes, creating a positive pressure inside the column, making the solutions flow through the columns

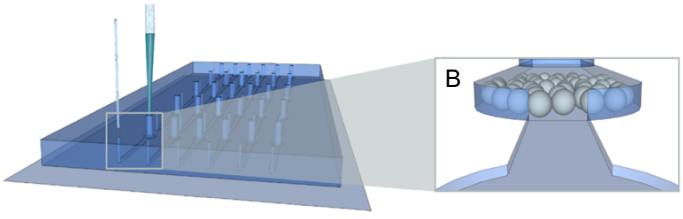

Figure 2: *Schematic representation of the bead packing mechanism. B) Bead trapping mechanism in the microfluidic channel.*

2.4 Image Analysis

All images were acquired using a Leica DMLM fluorescence microscope coupled to a DFC300FX camera. In this work two different fluorophores were used as labels, with different excitation and emission wavelengths, Cy3 and Atto-430LS. For the experiments using Atto-430 LS as a label, a blue excitation filter was used, with a band-pass excitation of 450-490nm and a long-pass emission of 510nm, and for the experiments using Cy3 as a label, a green excitation filter was used, with a band-pass excitation of 560/40nm and a long-pass emission of 595nm. Throughout this work the fluorescence signals were acquired under the same conditions, using a 10x magnification, gain of 1x, gamma of 1x and exposure time of 1 second. All images were analyzed using the ImageJ software (National Institute of Health, USA).

2.5 Optimization Experiments

The optimization experiments all followed very similar protocols. A 20μL solution of padlock probe (100nM) and padlock (250nM) is flown through the

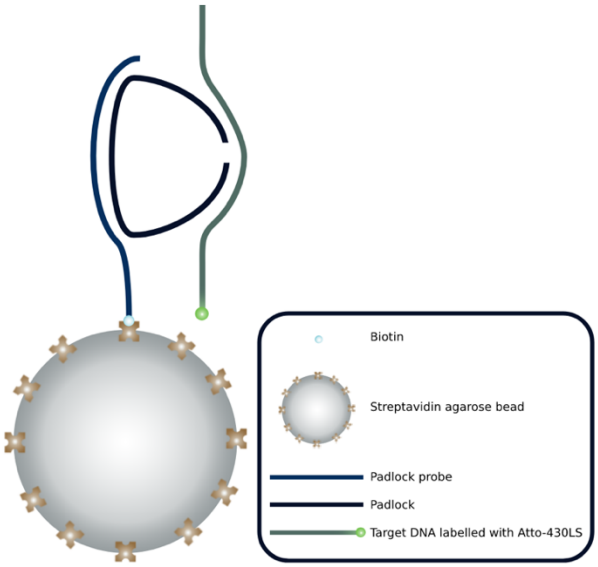

Figure 3: *Schematic representation of the target DNA capture. The padlock probe is bound to the streptavidin bead through the biotin-streptavidin bond and hybridized to the padlock, which in turn is hybridized to the target DNA.*

channel, followed by the target DNA labeled with Atto-430LS (250nM) which will hybridize to the immobilized padlock (Figure 2). After flowing all the solutions, a wash with PBS is performed to remove any unbound molecules at 5μL/min for 1min. In the flow rate optimization experiments, four different flow rates were tested for both steps of the experiment: 1.5μL/min, 1μL/min, 0.5μL/min and 0.25μL/min. When evaluating the target DNA capture under different saline conditions, the target DNA labeled with Atto-430LS was flown in three different 20μL solutions, aside from the standard buffer PBS. The first solution consisted of 1x T4 DNA Ligase Reaction buffer (SciLifeLab, Sweden) diluted in MiliQ water to make 20μL, the second solution contained Genolyse® Lysis Buffer (Hain Lifescience, Germany) and B-PER™ (Thermo Fischer Scientific, USA) in a ratio of 1 to 1, to make 20μL. Lastly, the third solution contained Genolyse ® Lysis Buffer and B-PER™ (in a ratio of 1 to 1) and Neutralization Buffer in a ratio of 2 to 1, to make 20μL.

2.6 Target DNA Capture Quantification

To quantify the target DNA capture using the developed assay, firstly, a calibration curve for the capture of a range of concentrations of Atto-430LS labeled target DNA on Q-Sepharose beads was created.

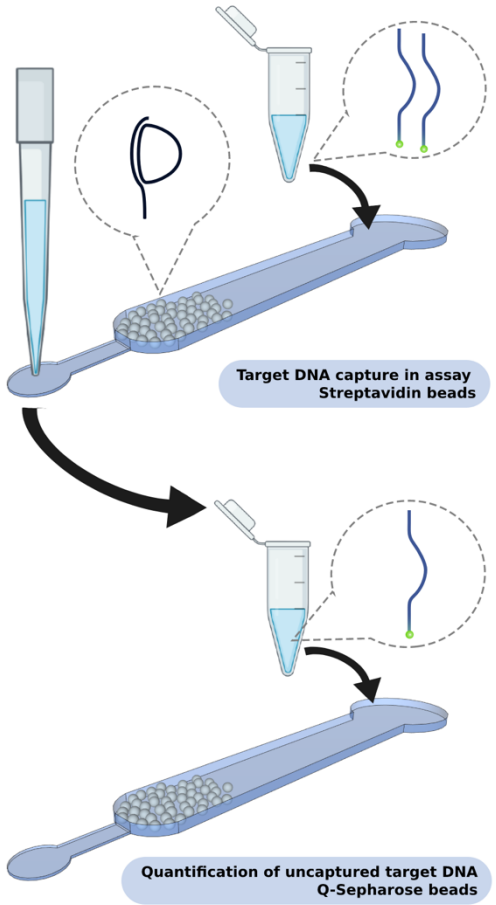

Figure 3: *Schematic representation of the mass balance calculation experiments. The target DNA capture assay is first performed on streptavidin beads. After flowing the Atto-430LS labelled target DNA solution through the channel it is collected at the outlet and flown through a second channel packed with Q-Sepharose beads.*

The experiments performed to obtain the calibration curve consisted of packing the channel with Q-Sepharose beads, preforming a wash with PBS at 5μL/min, followed by flowing the target DNA labelled with Atto-430LS at 0.5μL/min for 40min. With this calibration curve it is then possible to quantify the target DNA capture using a mass balance methodology, described in detail elsewhere. [25][26] This consisted of performing the target DNA capture assay described above (Figure 3), using a flow rate of 0.5μL/min for several concentrations of the Atto-430LS labelled target DNA (250nM, 100nM, 50nM and 10nM). After performing the target DNA capture assay the remaining target DNA solution was collected at the outlet and flown through a second channel packed with Q-Sepharose beads at 0.5μL/min in order to capture the remaining target DNA.

As the signal intensity on the Q-Sepharose beads is proportional to the mass of the target DNA, the mass of DNA hybridized to the padlocks can be obtained by equation 1:

$$m(DNA)_{padlock} = m(DNA)_{in} - m(DNA)_{Q-sepharose\ beads} \quad (1)$$

Where $m(DNA)_{in}$ is the known mass of DNA initially introduced into the first channel, and $m(DNA)_{Q-sepharose\ beads}$ is calculated by measuring the signal intensity of the target DNA present in the channel packed with Q-Sepharose beads after exiting the first channel (where the capture assay was performed) and correlating this signal with the calibration curve.

2.7 Rolling Circle Amplification

The channel is packed with Streptavidin beads, followed by a wash with PBS at 5μL/min for 1min. The microfluidic structure is then placed onto a hotplate and kept at 37℃ throughout the remainder of the assay. The channel walls are then blocked by flowing 4% BSA (Sigma-Aldrich, USA) at 2.5μL/min for 10min, followed by the immobilization of the biotinylated padlock probe (100nM) and padlock (250nM) on the beads by flowing the solution at 0.5μL/min for 40min. The target DNA is then flowed through the channel at 0.5μL/min in PBS. After the target DNA is hybridized with the padlock, a ligation solution with T4 DNA ligase enzyme (SciLifeLab, Sweden) (0.2U/ μL), ATP (0.5mM) (Thermo Fischer Scientific, USA), BSA (0.04%) as well as the T4 DNA ligase reaction buffer (1X), diluted with MiliQ water is flowed through the channel at 0.5μL/min for 40min, followed by an amplification solution with Phi29 polymerase enzyme (0.5U/μL) (SciLifeLab, Sweden), dNTPs (0.4mM) (SciLifeLab, Sweden), and BSA (0.053%) diluted in MiliQ water at 0.25μL/min for 60min. The Cy3 or Atto-430LS labelled detection oligonucleotides diluted in hybridization buffer (500nM) are then flowed trough the channel at 2μL/min for 15min followed by a wash with hybridization buffer (1.4 M NaCl, 0.01% TWEEN® 20, 20 mM of Tris-HCl, pH 8 and EDTA) at 2.5μL/min for 2min. Lastly, an additional wash with PBS at 5μL/min for 1min is performed.

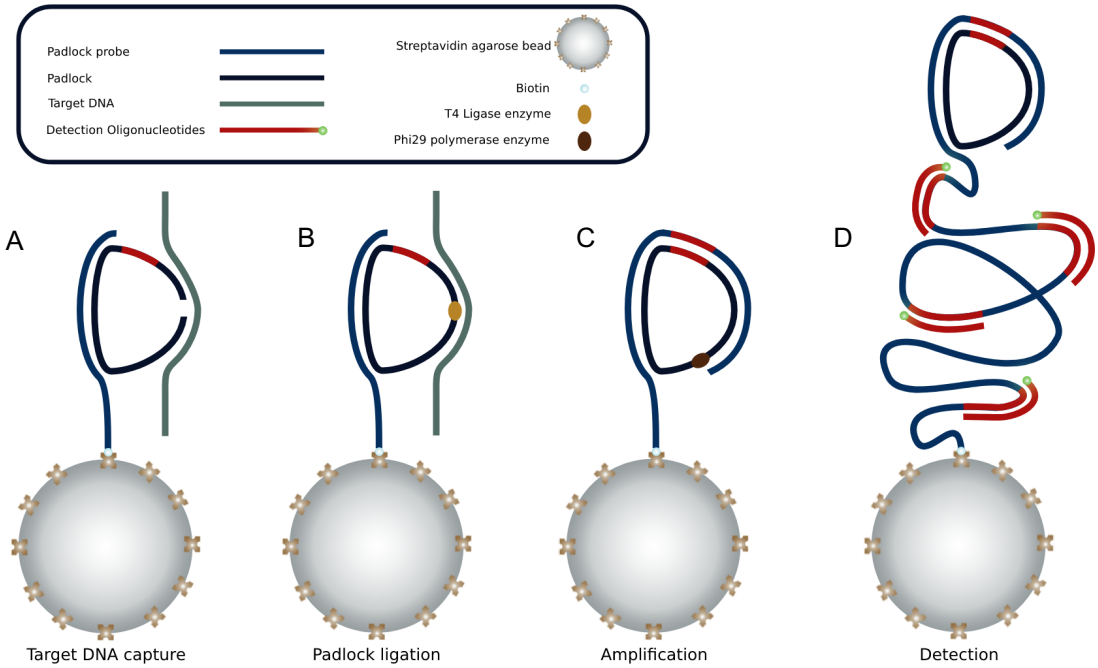

Figure 4: *Schematic representation of the RCA assay. A) Capture of the padlock probe on the streptavidin beads, hybridization with the padlock and the target DNA. B) Ligation of the padlock with T4 ligase. C) Amplification of the complementary padlock sequence using the phi29 polymerase. D) Detection of the amplified product by hybridizing Atto-430LS labeled detection oligonucleotide sequence with highlighted section of the amplified sequence*

3. Results and Discussion

3.1 Flow rate optimization

Four different flow rates were tested, 0.25μL/min, 0.5μL/min, 1μL/min and 1.5μL/min, and the results are presented in Figure 5A. It is noticeable that there is a large difference between the two higher flow rates (1.5μL/min and 1μL/min) and the two lower ones (0.25μL/min and 0.5μL/min), but that the difference between either the two higher flows and the two lower ones is very small, particularly when taking into account the variability of the experiment. These results can be explained by the fact that even though the transport in the microchannel occurs mainly through diffusion, due to the pumping system that is used in these experiments, convective transport in the direction of the fluid flow also has to be considered, particularly when different flow rates are being compared. As the DNA diffusion coefficient is very small, when flowing DNA through a microchannel, the Peclet number is often greater than 1, and particularly with higher flow rates, the convective transport becomes more relevant than diffusion. Therefore, with higher flow rates a large number of the target DNA molecules will pass over the immobilized padlock probe and padlock instead of diffusing into them and hybridizing, leading to a reduced capture of the target DNA. [27] The similarity between both higher flow rates can be explained by the fact that in both cases the rate between convective and diffusive transport, although higher for a 1.5μL/min flow rate, may be very similar. The same principle applies for the similarity between both lower flow rates, as the diffusive transport becomes more relevant for the 0.25μL/min than the 0.5μL/min flow rate. Therefore, the hybridization becomes again limited due to the fact that the padlock probe and padlock have to slowly diffuse through the channel, to hybridize and bind to the beads, as well as target DNA to the immobilized padlocks, even though the rate between convective and diffusive transport is very similar. Hence, the flow rate of 0.5μL/min provided the highest target DNA capture, due to the optimal compromise between convective and diffusive transport it allows and was the chosen flow rate to perform the following experiments.

3.2 Saline conditions

Given that the end-goal of this project is to have an integrated device in which to insert a sample collected at the time of the assay, extract the DNA and amplify it, the target DNA capture was evaluated under several saline conditions. These are related to cell lysis to extract the bacterial DNA and its amplification. To extract the bacterial DNA, a microfluidic chemical cell lysis module was developed in previous work [28] in which the Genolyse ® DNA extraction kit is used together with B-PER™. To understand if the extracted DNA could be directly captured in the device after cell lysis, the target DNA was mixed in solutions of lysis buffer and B-PER™, as well as lysis buffer, B-PER™ and neutralization buffer and flown through the microfluidic channel with the padlock probe and padlock previously immobilized on the beads. To amplify the extracted DNA, using the previously developed RCA protocol, the T4 DNA ligase enzyme requires a reaction buffer in order to optimize its activity. As another alternative to capture the DNA in an integrated device would be to clean the solution after cell lysis and flow the target DNA in the ligation solution which contains the T4 DNA ligase mixed in its reaction buffer and MiliQ water, this was also evaluated.

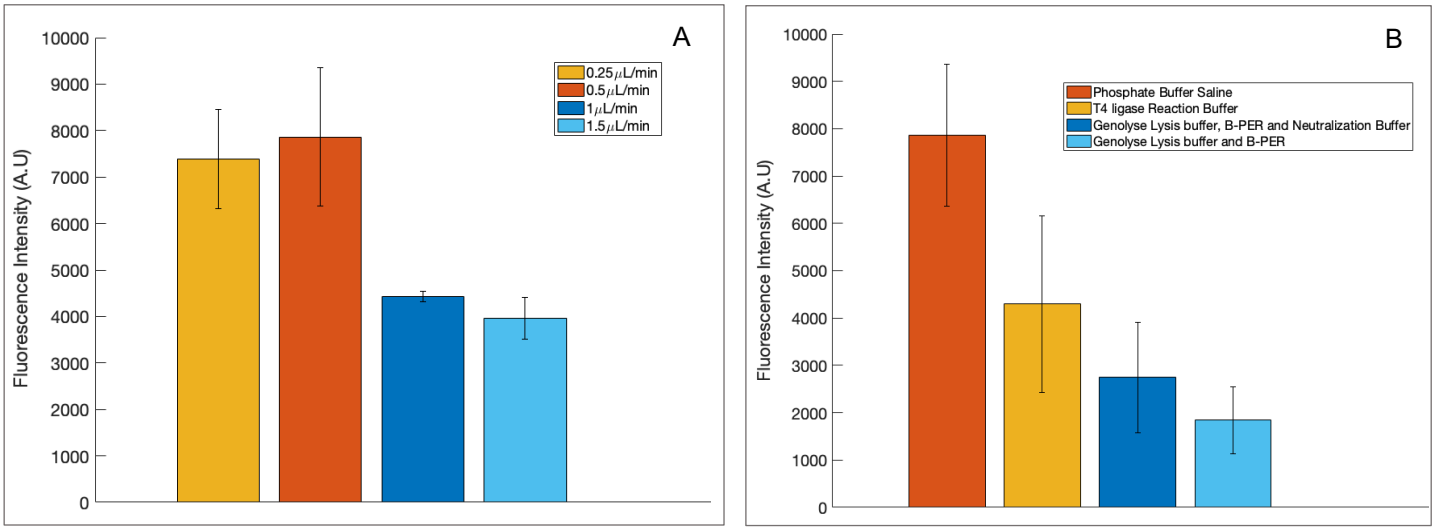

Figure 5: *A) Flow rate optimization for the capture of the target DNA. B) Effects of saline conditions on the Target DNA capture. The error bars in the graphic are the standard deviation of the measured signal of two experiments.*

The results are presented in Figure 5B, and it is noticeable, that as expected, using PBS as the buffer for the target DNA hybridization with the padlock provided the best results. This is due to the fact that DNA hybridization is affected by multiple factors, which include pH and salt concentrations.

Regarding the ligation solution, containing $2\mu L$ of reaction buffer and $13\mu L$ of MiliQ water, it is safe to assume that the salt concentrations will be lower since MiliQ water has very few ions, and the T4 DNA Ligase reaction buffer is very diluted. Given that DNA possesses negative charges along the phosphate backbone, which pose an electrostatic barrier for hybridization to occur, the presence of salts in the solution helps to mask those charges, reducing the electrostatic repulsions, and allowing DNA strands to approach with lower energies. Since the ligation solution has lower salt concentrations, it becomes harder for DNA to hybridize, giving rise to higher stringency conditions, decreasing the capture of the target DNA.

Regarding both lysis solutions, the dominant effect responsible for the lower signal is the pH, since the optimal pH for DNA hybridization and duplex stability is physiological pH, and lysis buffers act by increasing the pH (usually between 11.5 and 12.5 [29]) to break the cell membrane. The increase in pH makes the DNA bases become more hydrophilic and soluble, making it more difficult for them to interact with complementary bases, destabilizing the duplex. This is coherent with the results, especially given that when the neutralization buffer, which is supposed to decrease the pH, is added to the solution the signal increases slightly, compared with the lysis solution with no neutralization buffer.

Lastly, although the target DNA capture is less efficient in both the lysis and ligation solutions than in PBS, it is still possible to capture it in all of them, indicating that in an integrated device it might not even be necessary to clean the solution after cell lysis, which would complicate the process and make it more time-consuming.

Additionally, to evaluate the specificity of the developed assay under the conditions to which it may be subjected to upon integration with the cell lysis module, the target DNA capture assay was also performed with DNA strands non-complementary (ncDNA) to the padlock. The experiment was performed for 2 different ncDNA strands, one of which is from *S. Aureus* and has a slightly higher similarity with the padlock than the second ncDNA strand (23.7% and 19.8%, respectively).

The results are presented in Figure 6, and it is clear that the hybridization is significantly inhibited for both non-complementary target DNAs, although the *S. Aureus* ncDNA presents a slightly higher fluorescence signal, this increase is very small when taking into account the variability of the experiment, and the massive difference between both the ncDNAs and the cDNA fluorescence signals.

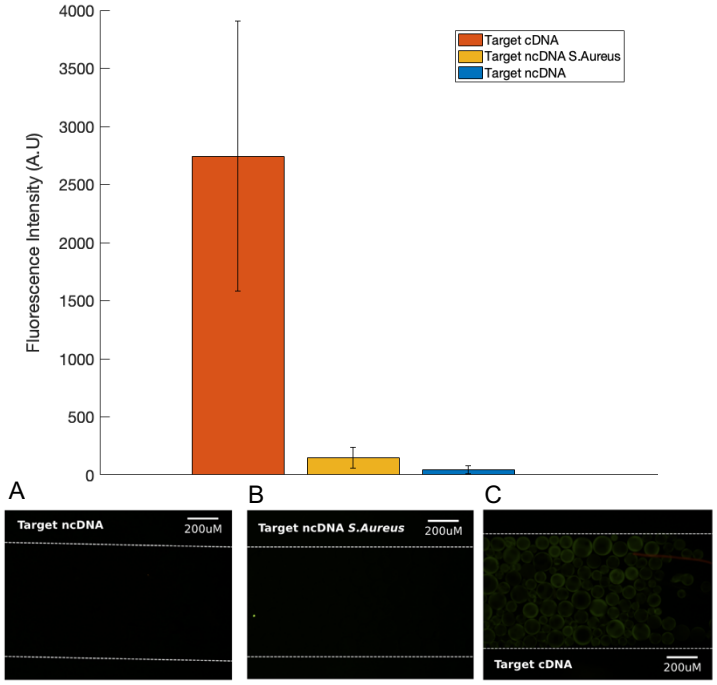

Figure 6: *Specificity of the target DNA capture assay. The error bars in the graphic are the standard deviation of the measured signal of two experiments. A) B) and C) Experimental images for the target DNA capture with ncDNA, S.Aureus ncDNA and cDNA in lysis solution, respectively. (Leica DMLM microscope, Exposure time: 1s, Gain: 1X, Magnification: 10X)*

3.3 Target DNA capture quantification

The calibration curve for the electrostatic target DNA immobilization on Q-Sepharose beads, represented in Figure 7, was created using a linear fit for

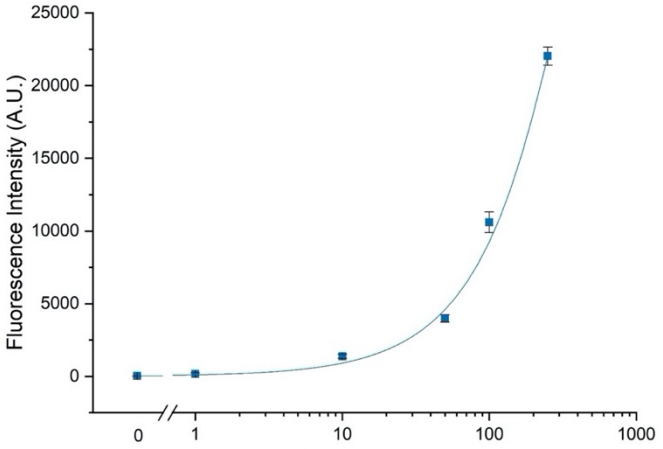

Figure 7: *Calibration curve for the capture of the Atto430-LS labelled target DNA on Q-Sepharose beads. The equation represents the linear regression that fits the data. The error bars in the graphic are the standard deviation of the measured signal of two experiments.*

the data, as for the range of concentrations used the fluorescence signal decreases linearly with the concentration.

The fluorescence signal measurements for the target DNA capture assay, as well as the fluorescence signal from the remaining target DNA captured on the Q-Sepharose beads for all target DNA concentrations tested are presented in Figure 8A. It is possible to see that the signals for the 250nM and 100nM target DNA capture assay are very similar, and particularly that the fluorescence signal for the capture of the remaining 250nM target captured on the Q-Sepharose beads is quite high. This indicates that for the highest target DNA concentration the capture isn't very efficient. However, given that the concentrations of padlock probe and padlock introduced into the channel are quite similar to that of the target DNA and that not all molecules might have been immobilized on the beads, the padlocks might be becoming saturated with target DNA at lower concentrations than the 250nM. This becomes more evident as the concentrations are lowered, and the ratios between the signals of the first and second channel increase. This is made evident in Figure 8B as the fluorescence emitted in the target DNA capture assays is somewhat similar for the 3 concentrations (250nM, 100nM and 50nM), but the fluorescence in the channel with the Q-Sepharose beads decreases significantly with the concentration.

As previously stated, the signal intensity on the Q-Sepharose beads was proportional to the mass of the target DNA and thus, the mass of DNA hybridized to the padlocks can be obtained by equation 1, where $m(DNA)_{in}$ is the known mass of DNA initially introduced into the first channel, and $m(DNA)_{Q-sepharose\ beads}$ is calculated by measuring the signal intensity of the target DNA present in the channel packed with Q-Sepharose beads after exiting the first channel (where the capture assay was performed) and correlating this signal with the calibration curve in Figure 7.

It was possible to calculate the number of target DNA molecules captured in the assay for the entire range of concentrations that were tested: $1.335 \times 10^{-12} \pm 5.294 \times 10^{-14}$mol, $1.059 \times 10^{-12} \pm 6.909 \times 10^{-14}$mol, $7.675 \times 10^{-13} \pm 5.951 \times 10^{-14}$mol to $2 \times 10^{-13} \pm 0$mol, for the initial target DNA concentrations of 250nM, 100nM, 50nM and 10nM, respectively. For a concentration of 250nM of target DNA only 27% was captured during the assay, increasing for smaller concentrations, with capture efficiencies of 53%, 77%

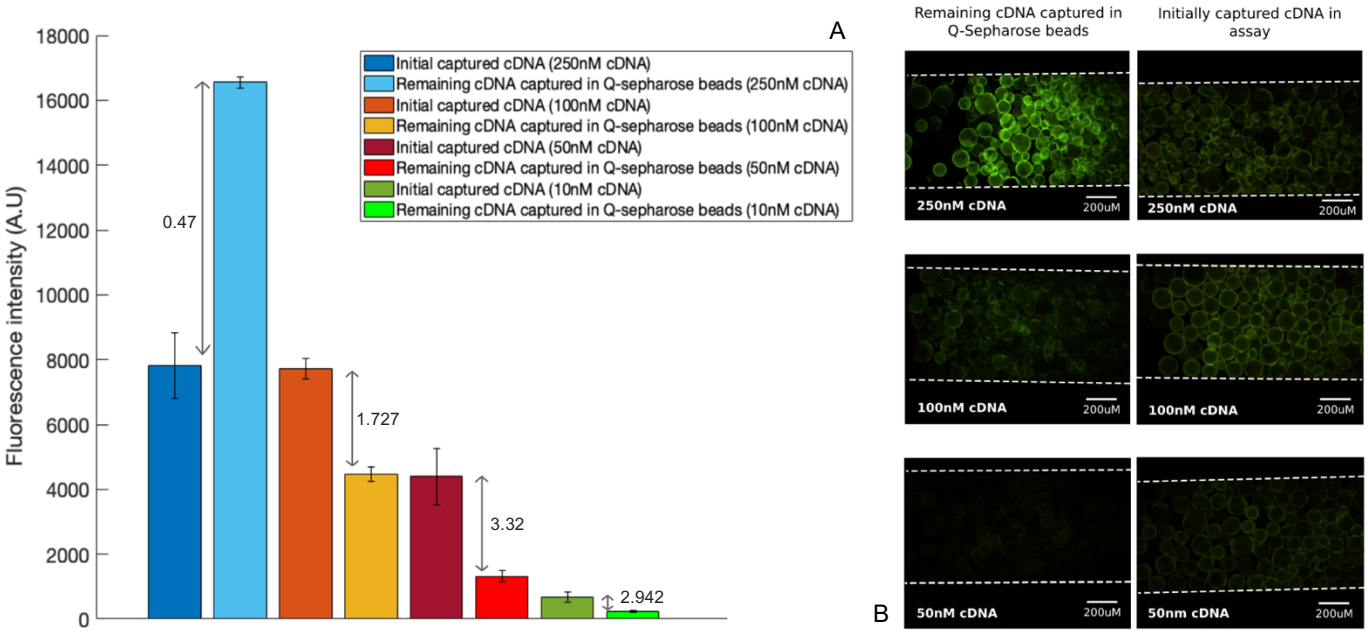

Figure 8: *Mass balance calculation experiments. A) The darker colored bars represent the uncaptured target DNA and the lighter colored bars represent the captured target DNA. The error bars in the graphic are the standard deviation of the measured signal of two experiments. Presented next to the bars are the ratios between the target DNA captured during the assay and the uncaptured target DNA. B) Experimental images of the mass balance calculation experiments. On the left are the images of the Q-Sepharose beads packed channels and on the right are the images of the target DNA capture assay.*

and virtually 100% for 100nM, 50nM and 10nM, respectively. However, the fluorescence signal emitted by the remaining 10nM target DNA solution in Q-Sepharose beads ($\sim 236A.U$) compared to the fluorescence signal to when no target DNA is present on the beads ($\sim 26A.U$) is around 12 times higher, indicating that there still is a certain amount of DNA that was not captured during the assay. This highlights that although the calculated efficiency for the capture of the 10nM target DNA concentration was 100%, there is an associated error to the calculations performed from the calibration curve, as well as limitations inherent to the microscope's sensitivity that don't allow to accurately quantify the capture efficiency for lower concentrations.

Although higher target DNA capture efficiencies (95.3% to 97.3% for target DNA concentrations above 3nM) have been reported in the literature, for a similar capture system, using probes immobilized on beads no further optimization was done to the capture assay. [25] This is because although similar, the reported method relied only on an already immobilized probe for the target DNA to hybridize to, while in this assay the padlock immobilization is additionally dependent on the padlock probe binding to the beads through the streptavidin-biotin interaction as well as the padlock hybridizing to the probe. Therefore, it is reasonable to assume that the capture is somewhat less efficient due to the multitude of factors that influence it.

3.4 Rolling circle amplification

The RCA assay was performed for a 10nM and 1nM concentration of target DNA, as well as a control with no target DNA, using the Atto-430LS labeled detection oligonucleotides to detect the amplified products. The results are presented in Figure 9 as well as the fluorescence signal for the capture of 10nM of target DNA, and it is possible to see that the fluorescence signal emitted by just the captured 10nM target DNA is around 15 times lower than the signal after amplification. This highlights the fact that the amplification is indeed occurring in the microfluidic channel.

It has been reported in the literature that the Phi29 enzyme can amplify a 100bp padlock into a complementary concatemer with approximately 1000 copies in 1hour. [23] Therefore, to understand if the proposed assay's yield is similar to that reported in literature, several calculations were performed in order quantify the fluorescence signal. Firstly, from the calibration curve in Figure 7 it is possible to estimate how much signal a single Atto-430LS labelled molecule would emit, which is around 7.85×10^{-9}A.U. From there, assuming 100% capture of the 10nM target DNA, and given that only padlocks that are hybridized to the target are circularized and can be amplified, there would be 1.204×10^{11} padlocks available for amplification. Assuming the 1000-fold amplification reported in the literature, and that each padlock only has one repetition of the sequence complementary to the detection oligonucleotides there would be 1.204×10^{14} padlock copies to which the detection oligonucleotides can hybridize to. This should result in a fluorescence signal around 945704A.U, which is lower than the signal that was obtained. Applying the same reasoning for the RCA initiating from 1nM of target DNA, after amplification, the

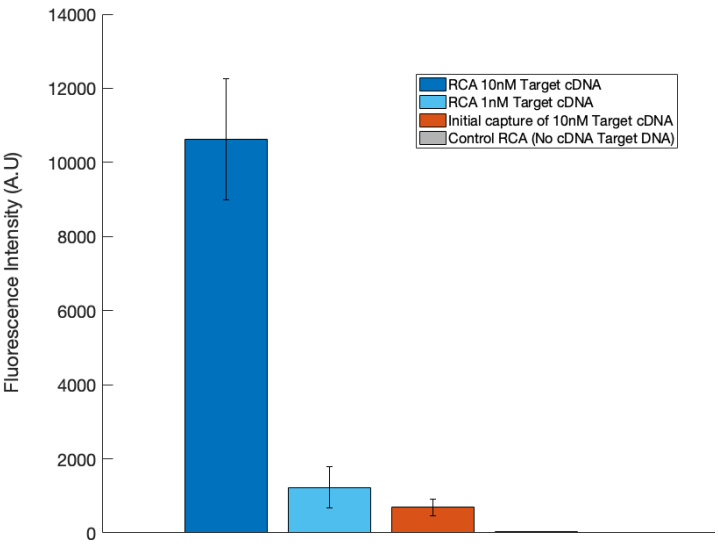

Figure 9: *Capture and rolling circle amplification of 10nM of target DNA, rolling circle amplification of 1nM of target DNA and control for the RCA assay. The error bars in the graphic are the standard deviation of the measured signal for two experiments.*

fluorescence signal should be around 94570.4A.U, which is again lower than the signal obtained in the experiment. From the signals obtained in both experiments and using the estimated value for the fluorescence signal of a single fluorophore, the number of detected products is 1.35×10^{12} and 1.56×10^{11} for the 10nM and 1nM target DNA concentration, respectively. This accounts for approximately 1% detection of the amplified products. It has been reported that the amplification performing the RCA assay using beads in a microfluidic channel results in a detection rate of around 8% [21] which is quite higher than the one obtained for the developed assay. However, it is still superior to a previously reported detection rate of 0.02%, performing the RCA in solution and detecting the amplification products in a microchip. [21]

From these results it would be reasonable to conclude that the RCA assay could be further optimized. However, it must be taken into consideration that this assay was performed under continuous flow, while the RCA assay where the detection rate of 8% was achieved the ligation and amplification steps were performed in a stationary fashion. Additionally, the detection oligonucleotide solution was flown in the microfluidic channel followed by a 20min incubation. This in conjunction with the different detection methodology used can be the reason for the higher detection rate. To

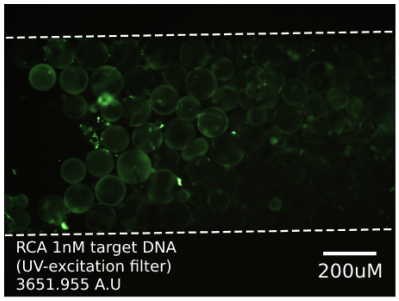

Figure 10: *Experimental image of the RCA assay with 1nM target DNA exciting the Atto-430LS detection oligonucleotides with a UV-Filter. (Leica DMLM microscope, Exposure time: 1s, Gain: 1X, Magnification: 10X)*

overcome this detection limitation one approach that was attempted was to excite the Atto-430LS labelled detection oligonucleotides with a UV-filter instead of the blue-filter used in the previous experiments. The results are presented in Figure 10 and is visible that just by changing the excitation wavelength the fluorescence signal is around 3 times higher. This could result in a higher rate of detection, in addition to allowing the detection of smaller concentrations of RCA products.

After optimizing both the capture and RCA assays, using a synthetic oligonucleotide sequence for the target DNA, the RCA assay was performed again, using *Staphylococcus Aureus* genomic DNA (4375copies/mL). The assay followed the previously mentioned RCA protocol, but flowing the genomic DNA in PBS at 60℃ for denaturation to occur. The detection of the amplified products was done using the detection oligonucleotides labelled with Cy3. The results are presented in Figure 10, and although the signal for the experiment with *S. Aureus* genomic DNA is slightly higher than the control, the difference between them is quite small when taking into account the experiments variability and therefore it is possible to conclude that the genomic DNA may not have been efficiently captured and amplified. Given that until now the target DNA sequence to be captured was quite small compared to the size of the *S. Aureus* genomic DNA (2.8Mbp) it is possible that due to its large size it may get trapped on the porous beads or just flow through the channel without hybridizing to the padlock. Another possibility was that the 60℃ may not be sufficient to denature the genomic DNA, and therefore the RCA assay was also performed denaturing the *S. Aureus* genomic DNA off-chip at 95℃ for 5min, followed by cooling in room-temperature water. However, as shown by the results in Figure 10 the signal is even lower than that for the RCA with on-chip denaturation at 60℃, showing that the most likely cause for no amplification occurring is that the *S. Aureus* genomic DNA is not being efficiently captured.

From these results it is possible to conclude that in order for complete integration with the microfluidic cell lysis chip, further optimization of the assay is necessary.

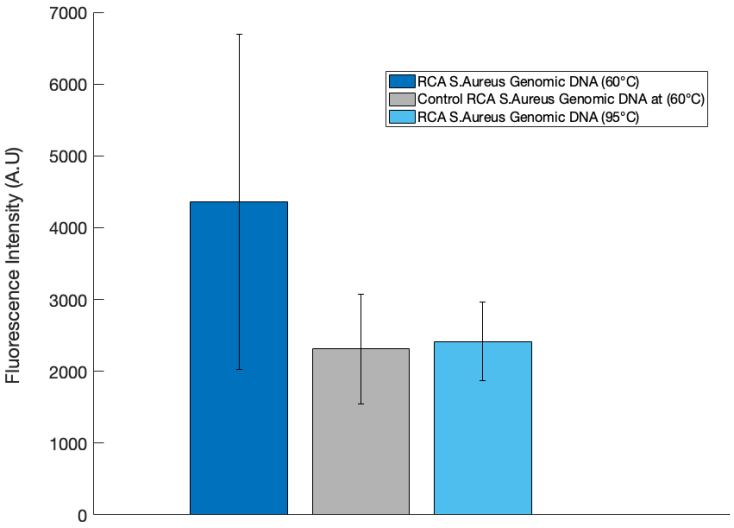

Figure 10: *Rolling circle amplification with Staphylococcus Aureus genomic DNA denaturing at 60℃ and 95℃, along with the control for the RCA assay denaturing at 60℃. The error bars in the graphic are the standard deviation of the measured signal for two experiments.*

The optimization will most likely include digesting the *S. Aureus* DNA with restriction enzymes so the sequence in the *S. Aureus* genome complementary to the padlock can more easily hybridize, followed by amplification. Additionally, since it is not clear whether steric hindrance caused by the large size of the genomic DNA is the single cause for the lack of target capture and amplification, several denaturation temperatures will also have to be tested. This is because, when using PDMS heating the device at 95℃ would cause the formation of air bubbles and the temperature would also be higher than the melting temperature of the padlock probe-padlock duplex, so a compromise would have to be made regarding the denaturation temperature used in the device.

4. Conclusions and Future Work

The proposed assay requires a padlock probe hybridized to a padlock immobilized on streptavidin beads, for capturing the target DNA prior to amplification through RCA. This capture was optimized regarding several aspects, such as the flow rates and saline conditions. Several flow rates were studied in order to understand which provided the highest capture efficiency, leading to the conclusion that smaller flow rates ($0.5\mu L$/min and $0.25\mu L$/min) resulted in a higher capture of the target DNA, due to the optimal compromise between convective and diffusive transport. Given that the end-goal of the project would be to have a device with integrated cell lysis, DNA capture, amplification and detection, the target DNA capture was also performed under different saline conditions. The capture was evaluated in 2 different lysis solutions, a ligation solution and PBS in order to understand if the RCA assay could be performed directly with the target DNA in the lysis solution or if purification would be required. Although the capture decreased in both lysis and ligation solutions when compared with the capture in PBS, it was still possible to capture the target DNA in all tested solutions. This indicates that purification of the sample after lysis may not be necessary, making the final device integration much easier, as well as more cost-effective.

Following the optimization, the target DNA capture was quantified using a mass-balance methodology. From these calculations, capture efficiencies ranging from 27% to 77% (250nM to 50nM of target DNA, respectively) were obtained, leading to the conclusion that the capture was more efficient for lower concentrations. Given that for pathogen detection the limit of detection for benchtop methods is around 10-1000 CFU/mL the goal for this module is to effectively capture low DNA concentrations, and therefore no further optimization was made to the target DNA capture assay. [30]

Using the optimized target DNA capture, the RCA assay was performed for concentrations of 10nM and 1nM of target DNA. As expected, the signal decreased around 10-fold with the decrease in concentration of target DNA. Although this assay has been optimized regarding several aspects, the RCA assay could still be further optimized in order to obtain a higher yield, given that the percentage of detectable products is lower than previously reported in literature for

a similar method. [52] However, further investigation is required in order to understand if the lower percentage of detectable products is related with the assay itself or with the detection methodology, given that it was already noted that by exciting the Atto-430LS labelled detection oligonucleotides with a UV-filter instead of the blue-filter results in a higher fluorescence signal. Furthermore, with the current assay architecture it is still not possible to capture and amplify *Staphylococcus Aureus* genomic DNA. This can be due to a lack of efficient capture of the target, either due to inefficient denaturation or difficulty in hybridizing with the immobilized padlocks due to steric hindrance caused by the large size of the genomic DNA. To access this prior to capturing, the *Staphylococcus Aureus* genomic DNA could be subjected to digestion by restriction enzymes so that it would be easier for the target sequence to hybridize with the immobilized padlock with little interference. Simultaneously, several denaturation temperatures and times should also be evaluated to understand if the lack of ssDNA available to hybridize with the padlocks is due to inefficient denaturation. Ultimately, the chosen denaturation temperature and time will be a compromise between the 95℃, most commonly used for denaturation, and the melting temperature of the padlock probe-padlock duplex, as well as the temperature the PMDS device can withstand without the creation of air bubbles. Following the resolution of these current issues, the integration of this module with the cell lysis module should be possible, resulting in a true POC sample-in-answer-out type of device for *Staphylococcus Aureus* detection, that could then be adapted in order to detect other pathogens.

Acknowledgements:

This document was written and made publicly available as an institutional academic requirement and as a part of the evaluation of the MSc thesis in Biomedical Engineering of the author at Instituto Superior Técnico. The work described herein was performed at INESC MN (Lisbon, Portugal), during the period February-November 2021, under the supervision of Professor João Pedro Estrela Rodrigues Conde and Dr. Ricardo Jaime Pereira Rosário dos Santos.

References:

[1] U.S Centers for Disease Control and prevention. (2019). *Antibiotic Resistance Threats in the United States*.

[2] Prestinaci, F., Pezzotti, P., & Pantosti, A. (2015). Antimicrobial resistance: a global multifaceted phenomenon. *Pathogens and Global Health*, *109*(7), 309–318.

[3] C Reygaert, W. (2018). An overview of the antimicrobial resistance mechanisms of bacteria. *AIMS Microbiology*, *4*(3), 482–501.

[4] McGowan, J. E., & Tenover, F. C. (1997). CONTROL OF ANTIMICROBIAL RESISTANCE IN THE HEALTH CARE SYSTEM. *Infectious Disease Clinics of North America*, *11*(2), 297–311.

[5] Griffith, M., Postelnick, M., & Scheetz, M. (2012). Antimicrobial stewardship programs: methods of operation and suggested outcomes. *Expert Review of Anti-Infective Therapy*, *10*(1), 63–73

[6] Lee, A. S., de Lencastre, H., Garau, J., Kluytmans, J., Malhotra-Kumar, S., Peschel, A., & Harbarth, S. (2018). Methicillin-resistant Staphylococcus aureus. *Nature Reviews Disease Primers*, *4*(1)

[7] Sun, J., Huang, J., Li, Y., Lv, J., & Ding, X. (2019). A simple and rapid colorimetric bacteria detection method based on bacterial inhibition of glucose oxidase-catalyzed reaction. *Talanta*, *197*, 304–309

[8] Zheng, W., Sun, W., & Simeonov, A. (2017). Drug repurposing screens and synergistic drug-combinations for infectious diseases. *British Journal of Pharmacology*, *175*(2), 181–191.

[9] Shi, X., Kadiyala, U., VanEpps, J. S., & Yau, S. T. (2018). Culture-free bacterial detection and identification from blood with rapid, phenotypic, antibiotic susceptibility testing. *Scientific Reports*, *8*(1).

[10] Sista, R., Hua, Z., Thwar, P., Sudarsan, A., Srinivasan, V., Eckhardt, A., Pollack, M., & Pamula, V. (2008). Development of a digital microfluidic platform for point of care testing. *Lab on a Chip*, *8*(12), 2091

[11] Foudeh, A. M., Fatanat Didar, T., Veres, T., & Tabrizian, M. (2012). Microfluidic designs and techniques using lab-on-a-chip devices for pathogen detection for point-of-care diagnostics. *Lab on a Chip*, *12*(18), 3249

[12] Soares, R., Santos, D., Chu, V., Azevedo, A., Aires-Barros, M., & Conde, J. (2017). A point-of-use microfluidic device with integrated photodetector array for immunoassay multiplexing: Detection of a panel of mycotoxins in multiple samples. *Biosensors and Bioelectronics*, *87*, 823–831.

[13] Gardeniers, H., & den Berg, A. V. (2004). Micro- and nanofluidic devices for environmental and biomedical applications. *International Journal of Environmental Analytical Chemistry*, *84*(11), 809–819.

[14] Sia, S. K., & Whitesides, G. M. (2003). Microfluidic devices fabricated in Poly(dimethylsiloxane) for biological studies. *ELECTROPHORESIS*, *24*(21), 3563–3576.

[15] Soares, R. R. G., Akhtar, A. S., Pinto, I. F., Lapins, N., Barrett, D., Sandh, G., Yin, X., Pelechano, V., & Russom, A. (2021). Sample-to-answer COVID-19 nucleic acid testing using a low-cost centrifugal microfluidic platform with bead-based signal enhancement and smartphone read-out. *Lab on a Chip*, *21*(15), 2932–2944.

[16] Chang, C. M., Chang, W. H., Wang, C. H., Wang, J. H., Mai, J. D., & Lee, G. B. (2013). Nucleic acid amplification using microfluidic systems. *Lab on a Chip*, *13*(7), 1225.

[17] Ahrberg, C. D., Manz, A., & Chung, B. G. (2016). Polymerase chain reaction in microfluidic devices. *Lab on a Chip*, *16*(20), 3866–3884.

[18] Xiang, Q., Xu, B., Fu, R., & Li, D. (2005). Real Time PCR on Disposable PDMS Chip with a Miniaturized Thermal Cycler. *Biomedical Microdevices*, *7*(4), 273–279.

[19] Hataoka, Y., Zhang, L., Mori, Y., Tomita, N., Notomi, T., & Baba, Y. (2004). Analysis of Specific Gene by Integration of Isothermal Amplification and Electrophoresis on Poly(methyl methacrylate) Microchips. *Analytical Chemistry*, *76*(13), 3689–3693.

[20] Mahmoudian, L., Kaji, N., Tokeshi, M., Nilsson, M., & Baba, Y. (2008). Rolling Circle Amplification and Circle-to-circle Amplification of a Specific Gene Integrated with Electrophoretic Analysis on a Single Chip. *Analytical Chemistry*, *80*(7), 2483–2490.

[21] Sato, K., Tachihara, A., Renberg, B., Mawatari, K., Sato, K., Tanaka, Y., Jarvius, J., Nilsson, M., & Kitamori, T. (2010). Microbead-based rolling circle amplification in a microchip for sensitive DNA detection. *Lab on a Chip*, *10*(10), 1262.

[22] Ali, M. M., Li, F., Zhang, Z., Zhang, K., Kang, D. K., Ankrum, J. A., Le, X. C., & Zhao, W. (2014). Rolling circle amplification: a versatile tool for chemical biology, materials science and medicine. *Chemical Society Reviews*, *43*(10), 3324.

[23] Soares, R. R. G., Madaboosi, N., & Nilsson, M. (2021). Rolling Circle Amplification in Integrated Microsystems: An Uncut Gem toward Massively Multiplexed Pathogen Diagnostics and Genotyping. *Accounts of Chemical Research*.

[24] Pinto, I., Caneira, C., Soares, R., Madaboosi, N., Aires-Barros, M., Conde, J., Azevedo, A., & Chu, V. (2017). The application of microbeads to microfluidic systems for enhanced detection and purification of biomolecules. *Methods*, *116*, 112–124.

[25] Caneira, C. R., Soares, R. R., Pinto, I. F., Mueller-Landau, H. S., Azevedo, A. M., Chu, V., & Conde, J. P. (2019). Development of a rapid bead-based microfluidic platform for DNA hybridization using single- and multi-mode interactions for probe immobilization. *Sensors and Actuators B: Chemical*, *286*, 328–336.

[26] Pinto, I. F., Santos, D. R., Caneira, C. R. F., Soares, R. R. G., Azevedo, A. M., Chu, V., & Conde, J. P. (2018). Optical biosensing in microfluidics using nanoporous microbeads and amorphous silicon thin-film photodiodes: quantitative analysis of molecular recognition and signal transduction. *Journal of Micromechanics and Microengineering*, *28*(9), 094004.

[27] Kim, J. H. S., Marafie, A., Jia, X. Y., Zoval, J. V., & Madou, M. J. (2006). Characterization of DNA hybridization kinetics in a microfluidic flow channel. *Sensors and Actuators B: Chemical*, *113*(1), 281–289.

[28] Caneira, C. R. F., Monteiro, S., Santos, R., Chu, V., & Conde, J. P. (2019, October). *A microfluidic module for integrated lysis and genetic material detection of gram-positive and gram-negative bacteria [Poster session]. MicroTAS, Basel, Switzerland.*

[29] Shehadul Islam, M., Aryasomayajula, A., & Selvaganapathy, P. (2017). A Review on Macroscale and Microscale Cell Lysis Methods. *Micromachines*, *8*(3), 83.

[30] Foudeh, A. M., Fatanat Didar, T., Veres, T., & Tabrizian, M. (2012). Microfluidic designs and techniques using lab-on-a-chip devices for pathogen detection for point-of-care diagnostics. *Lab on a Chip*, *12*(18), 3249.